Journal of Brilliant Engineering 2 (2025) 41007
Brilliant Engineering
journal home: www.acapublishing.com/journals/4/ben

Research Article

Sensitivity of Asphalt Overlay Thickness to Implication of Geogrids Reinforcement

Saad Issa Sarsam*,[1]
[1]Professor, Sarsam and Associates Consult Bureau (SACB), Baghdad-IRAQ. Former Head, Department of Civil Engineering, College of Engineering, University of Baghdad, Iraq

Keywords

Geogrids,
Asphalt concrete,
Overlay thickness, Deformation,
Sensitivity,
Load carrying capacity.

Abstract

The sensitivity of the overlay thickness to the implementation of geogrid is assessed using two types of biaxial geogrid (AR-G and AR-1). Circular Asphalt concrete specimens of 152.4 mm diameter and 38.1 mm thickness were constructed and denoted as the lower layer. The hot asphalt concrete material required to construct the upper layer (representing overlay) of variable thickness (38.1 and 63.5) mm was compacted over the lower layer specimen after inserting the geogrid in between. The coupled specimens were tested in a model box of 50 x50 x70 cm filled with loose sand layer of 40 cm thickness, and the load – deformation data was recorded. Implementation of geogrids (AR-1 and AR-G) in thin asphalt concrete layer (38.1 mm over 38.1 mm) improved resistance to deformation by (83.3 and 33.3) % and the load sustaining capacity declined by (19.2, and 23) % respectively as compared with the control mixture. For thick asphalt concrete layer, (63.5 mm over 38.1mm), the implementation of geogrids exhibited improved resistance to deformation by 11.2 % regardless of the geogrid type and the load sustaining capacity declined by (40, and 50) % when AR-1 and AR-G geogrids were implemented respectively as compared with the control mixture. The viscoelastic stage of failure for the thin layer of reinforced asphalt concrete was extended to 6 mm of punching deformation as compared with the control sample. However, the thick layer of reinforced asphalt exhibits no significant variation in the stages of failure.

1. Introduction

The implication of geogrids in asphalt concrete pavement exhibits a positive role in enhancing pavement performance by increasing the structural capacity and reducing distress potential. Geogrids have been extensively implemented as a pavement maintenance solution. Ibrahem et al., 2017 [1] assessed a pavement section with geogrids reinforcements placed at different positions within the pavement. The pavement sections were loaded with static plate-loading equipment. Results showed that geogrids can be used to reduce tensile stress in flexible pavement systems. It was concluded that the optimum position of the geogrid reinforcement to reduce tensile strains was found to be directly underneath the AC layer. Bekheet et al., 2019 [2] investigated the influence of varying the thickness of binder layer and the geogrid type used on the behavior of asphalt pavement. Two types of geogrids were used, Biaxial and Triaxial geogrids. Beam specimens were prepared and tested using three-point bending beam tests. Test results exhibited that introducing geogrid in asphaltic layers shows maximum force and lower deformation and the rate of crack propagation can be reduced. Albayati et al., 2023 [3] stated that geotextiles can significantly improve the overall performance of the asphalt concrete overlays. Overlays with geotextiles had improved the fatigue life of asphalt concrete by 97.8%, as compared with the reference mix. It was revealed that when increasing its thickness by 50 %, it can exhibit a noticeable improvement in the performance against reflection cracking and the fatigue life improved by 53.6 %. Zarei et al., 2025 [4] evaluated the influence of using different geogrids within the asphalt layer on controlling the cracking and rutting and extending the fatigue life in flexible pavements. Viscoelastic analyses of control and reinforced pavements were conducted using a three-dimensional finite-element model. The results indicate that placing geogrids, at the bottom or one-third of the asphalt concrete layer, significantly enhances pavement performance. Geogrids can reduce shear strain by 48.4 % and vertical compressive strain by 28.1 % and reduce transverse strains by 42 %. Albayati et al., 2024 [5] evaluated the effectiveness of geotextile fabric positioning at the base and at 1/3 depth of the asphalt concrete specimen. A clear enhancement was observed with geotextile incorporation. It was concluded that Geotextile placement, particularly at 1/3 depth, can contribute significantly to the energy required to initiate the crack. Mounes et al., 2016 [6] performed dynamic creep test on asphalt concrete samples reinforced with different types of fiberglass grids with two different sizes of grid openings and two tensile strengths. The results pointed out the importance of grid mesh size in controlling permanent deformation. Solatiyan et al., 2021 [7] assessed the mechanical properties of reinforced asphalt concrete with geogrid products, used as an interlayer with the aid of 3-Point Bending Test. The results revealed that reinforcement of the interface by geogrid products significantly enhances the fracture toughness of the flexible pavement in terms of bonding quality and crack resistance. Ingrassia et al., 2020 [8] assessed the influence of geocomposite reinforcement on cracking and permanent deformation accumulation of thin asphalt pavements with the aid of a full-scale trial section which was constructed with three types of geocomposite created by combining the grid with asphalt concrete. Significant permanent deformations were observed due to the plastic yielding of the unbound layers. However, the geocomposite improved the resistance to permanent deformation as compared with the control pavement. It was concluded that the use of geocomposite can extend the service life of thin asphalt pavements. Kumar et al., 2022 [9] conducted a series of loading on control and geosynthetic-reinforced asphalt overlays to monitor the increased in the roadway structural capacity. Monitoring tensile strains among the different test sections exhibited significantly smaller tensile strains in the geosynthetic-reinforced sections as compared with those obtained in the control section. It was concluded that grids provide added roadway structural capacity. Kumar et al., 2021 [10] investigated the influence of different geosynthetic reinforcements on the fatigue performance of asphalt concrete layers. Three different types of geosynthetic reinforcement were employed to

*Corresponding Author: saadisasarsam@coeng.uobaghdad.edu.iq
Received 27 May 2025; Revised 10 Jun 2025; Accepted 10 Jun 2025 https://doi.org/10.36937/ben.2025.41007
2687-5195 /© 2022 The Authors, Published by ACA Publishing; a trademark of ACADEMY Ltd. All rights reserved.

evaluate the fatigue behavior of asphalt concrete layers. Testing results indicated that incorporating geosynthetic reinforcement in the asphalt concrete layers had improved the fatigue performance by factors ranging (11, to 38) %. At failure, a maximum tensile strain of 11.2% was obtained in control specimens while it declines to a range of (2.7 to 3.8) % in geosynthetic-reinforced asphalt specimens. Xue et al., 2023 [11] evaluated the performance of the flexible pavements over a weak subgrade. The pavements were reinforced with three types of geosynthetic products. Different configurations of layer thickness, reinforcement's location have been adopted. Test results exhibited that there is a large variation in the properties of the structures. Smaller plates are recommended when determining the modulus of thin base course layers used to minimize the influences from the subgrade. Gallage et al., 2024 [12] constructed series of model pavements within a steel box. Various parameters, including subgrade stiffness, and geosynthetic types, were assessed during the construction of these models. The static plate load tests were conducted in a controlled laboratory environment. The test results provided valuable insights into the overall stiffness of the reinforced subgrade. It was concluded that the incorporation of geosynthetics can reduce the overall granular cover thickness by approximately 20%. Sarsam, 2013 [13] investigated the properties of biaxial geogrid reinforced asphalt concrete. It was revealed that thicker geogrids ribs exhibit better reinforcing performance when compared with thinner rip thickness of the grid. Prakash and Rathod, 2024 [14] presented an overview of products like geogrid, as well as their interactions with different pavements. The load transfer mechanism in geogrid, and the optimal placement of these materials can improve load-carrying capacity and reduce surface deformations. Kumar et al., 2022 [15] evaluated the performance of geogrid reinforced asphalt overlays. Two layered asphalt concrete beam specimens were tested under repeated four-point bending beam conditions. The performance of the different geogrid-reinforced specimens was compared against that of the control specimen and the improvement in fatigue life was evaluated. It was concluded that all the geogrid-reinforced specimens exhibited an extended fatigue life of overlays as compared with the control mixture. Luan et al., 2023 [16] assessed pavement condition of four projects and the cracking pattern and amount were monitored before and after asphalt overlaying. The Finite Element Method of analysis was conducted to study the effects of existing pavement conditions on cracking resistance of a new overlaying. The new overlaying strategy was proposed to control the reflective crack, in which geogrid is employed and inserted between the existing pavement layer and the bottom layer of overlay. Patil1, and Shivananda, 2017 [17] assessed the functioning of geogrids with various axial stiffness values in flexible pavement through finite element analysis. Reduction in the vertical deformation was observed with four folds increase in stiffness of geogrid. The vertical deformation of geogrid reinforced pavement under dual wheel load is lower than that of control sample. Asadi and Shafabakhsh, 2023 [18] investigated the influence of geocomposite tensile strength and bending fatigue loading frequency on asphalt overlays performance. It was noticed that at the high loading frequency (more than 10 Hz), increasing the temperature from 0 to 20 and 40 °C will increase the crack growth rate between 5 and 30 times for reinforced mixture. High coefficients of determination indicate the satisfactory prediction of the model as compared with the real observations. Rueda et al., 2023 [19] evaluated the influence of geogrids as a reinforcement to asphalt mixture paving layers. Two types of large-scale samples (with and without reinforcement) were subjected to a monotonic load under two support conditions (simple support and granular base). The load- displacement was monitored and analyzed for parameters such as displacement, stiffness, peak load, and work of fracture. The results exhibited that the reinforcement in asphalt concrete layer with geogrid can strongly impact the mechanical behavior, and increasing the service life of the pavement.

The aim of the present work is to assess the sensitivity of asphalt concrete overlay thickness to implication of two types of biaxial geogrids (AR-1 and AR-G) as interlayer. The overlay mixture with (38.1 and 63.5) mm thickness will be compacted over a prepared circular specimens of asphalt concrete after inserting the geogrids in between. Specimens will be tested under static load bearing test in a model box filled with loose sand which represents the poor subgrade. The changes in the viscoelastic properties of asphalt concrete in terms of the load carrying capacity, stiffness, and the resistance to punching deformation under static load will be evaluated under variable overly thickness of the control and grid-reinforced asphalt concrete specimens using a unique testing setup for the experimental program.

2. Materials and Methods

2.1. Aggregates

Combiner coarse and fine aggregates were obtained from Al-Nubai, Mineral filler with 95 % finer than 75 micron was obtained from Karbala quarry; the physical properties are illustrated in Table 1. The testing was conducted as per the ASTM, 2015 procedure.

Table 1. Physical properties of aggregates according to ASTM, 2015 [20] testing procedures

Property	Coarse aggregate	Fine aggregate	Mineral filler	ASTM Designation
Specific gravity	2.680	2.620	2.640	ASTM C-127 and C-128
Absorption (%)	0.4	0.7	Not applicable	ASTM C-127 and C-128
Percent Wear (Los-Angeles Abrasion)	19.6	Not applicable	Not applicable	ASTM C-131

2.2. Asphalt cement binder

Asphalt cement binder of penetration grade (40-50) was obtained from Dorah refinery; the properties are as illustrated in Table 2. The testing was conducted as per the ASTM, 2015 [20] procedure.

Table 2. Properties of Asphalt cement according to ASTM, 2015 [20] testing procedures.

Property	Test results	ASTM Designation
Penetration (0. 1 mm)	48	ASTM D-5
Softening point (°C)	49	ASTM D-36
Ductility (cm)	+100	ASTM D-113
Specific gravity	1.024	ASTM D-70

2.3. Geogrids

Two types of Tensar biaxial geogrids have been implemented; Table 3 illustrates their properties.

Table 3. Tensar biaxial geogrids reinforcement's properties (as supplied by the manufacturers)

Type of geogrid	AR-G	AR-1
Unit weight	0.25 gm./ m^2	0.24 gm./ m^2
Transverse strength	20 kN/ m	18 kN/ m
Longitudinal strength	17 kN/ m	14 kN/ m
Thickness	1.2 mm	0.8 mm
Aperture size	60x76 mm	51x71 mm
Polymer	Polypropylene	Polypropylene

2.4. Preparation of Asphalt concrete mixture

Coarse and fine aggregates were mixed with mineral filler, the combined aggregates fall within the lower and upper limits of the SCRB, 2003 [21] specifications for wearing course pavement layer. The combined aggregates were heated to 160 ◦C then the required amount of asphalt cement binder which was heated to 150 ◦C was added and mixed thoroughly to create homogeneous asphalt concrete using mechanical mixer for 120 seconds. Table 4 presents the properties of the design asphalt concrete implemented.

Table 4. Properties of the Asphalt concrete wearing course mixture

Properties of asphalt concrete mixture	Test results	ASTM Designation
Optimum asphalt binder content (%)	4.8	ASTM-D-2172
Maximum theoretical specific gravity (Gmax)	2.482	ASTM D-2041
Marshall stability (kN)	10.1	ASTM D-6927 – 15
Marshall flow (mm)	2.8	ASTM D-6927 – 15
Specific gravity at optimum asphalt content	2.290	ASTM D-1188
Volume of voids (%)	4.9	ASTM D-2041
Voids filled with asphalt binder (%)	78	ASTM D-2041

Figure 1 exhibits the combined aggregates gradation. The maximum size of aggregate was 19.5 mm, and the nominal maximum size was 12.5 mm which was implemented for the mix design. The mixing temperature was maintained to 160 ˚C.

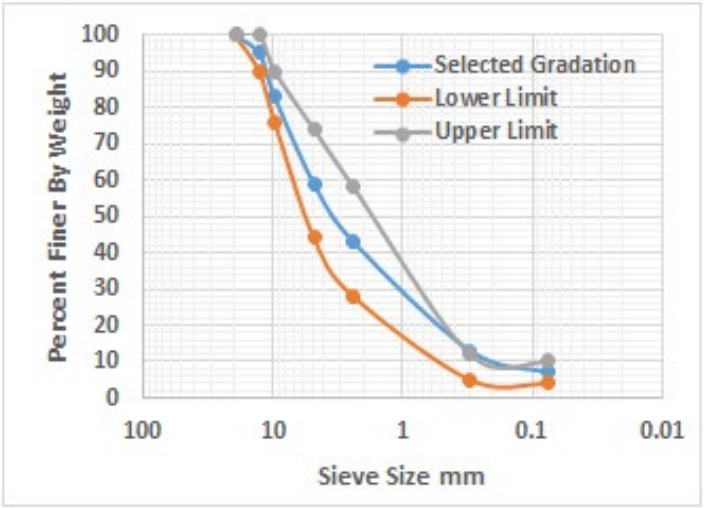

Figure 1. Combined gradation of asphalt concrete

2.5. Preparation and testing of Asphalt concrete Specimens

Asphalt concrete specimens of 152.4 mm diameter and 38.1 mm thickness were constructed using the traditional CBR mold and spacers, the required amount of hot Asphalt concrete mix (at 160 ˚ C) which gives the predetermined density of (2.290 gm / cm^3) at optimum asphalt content of 4.8 % was weighted, spread into the preheated mold, and subjected to initial compaction through a 50 spatula strikes, then the specimens were subjected to static compaction using Versa compression machine until the required specimen thickness was obtained at the target density, a total load of 5000 kg was required to achieve the target bulk specific gravity of (2.290). The specimens were compacted to 95 % of the maximum theoretical density. Filter papers have been introduced at the top and bottom faces of the specimens to prevent sticking to the spacers. Specimens were kept overnight to cool then withdrawn from the mold using hydraulic jack. For control specimens, the material required to construct the upper layer which represent the overlay with variable thickness (38.1 and 63.6) mm (when it was loose at 160 ^{0} C) was compacted over the pre compacted lower layer specimen which represent the existing pavement layer, this could simulate the field condition when constructing an overlay over existing pavement layer. The bonding between the upper and lower specimens is expected to occur due to the high compaction temperature rather than the need for a tack coat. However, for reinforced system, the material required to construct the upper layer (when it was loose at 160 ^{0} C) with variable thickness (38.1 and 63.6) mm was compacted over the pre compacted lower layer specimen after inserting the geogrid in between. The expected bonding between the upper and lower specimens and the geogrid occurs due to the high compaction temperature of 160 ^{0} C and interlock of aggregates with the geogrid rather than the need for a tack coat. Figure 2 exhibits the preparation, compaction, and the check of deformation of asphalt concrete cylindrical specimens with the aid of CBR molds and spacers.

Figure 2. Preparation and compaction of asphalt concrete specimens with the aid of CBR molds and spacers

Figure 3 shows the preparation of grid reinforced specimens with various types of reinforcements. The compaction temperature was maintained to 160 ˚C. The 50-Ton capacity compression machine was used for static compaction of the specimens and for testing the coupled specimens in the model box.

Figure 3. Preparation and testing of geogrid reinforced asphalt concrete samples

2.6. Testing of reinforced Asphalt concrete

The coupled specimens were transferred, centered, and seated into the testing box model of 50 x50 x70 cm dimensions on a layer of loose sand of 40 cm depth. The loose sand condition has been selected so that it could simulate compressible and poor subgrade, so that the reinforcing effect of asphalt concrete could be clearly detected. The loose sand was added into the model box by raining method. It was poured from height not exceeding 20 cm in layers, 100 mm for each layer until the desired height of sand was reached, and the layer was leveled with a straight edge. The sand is classified as poorly graded sand with a coefficient of uniformity (C_u)= 1.57 and coefficient of curvature (C_C) = 1. The maximum and minimum dry unit weight of sand are 17.4 kN/m^3 and 14.7kN/m^3 respectively and the specific gravity value of the used sand is 2.65. The load was applied through a circular metal plate of 10 mm thickness and 40 mm diameter using a strain-controlled system. An initial seating load of 10 Newton was applied consistently for all the tested specimens to ensure perfect contact between the plate and asphalt concrete top surface, also such contact was insured between the sub-grade sand and the bottom face of Asphalt concrete. The thickness of the overlay and the size of the loading plate were modelled to represent 50 % of the real field size (60 mm is the typical overlay thickness and 80 mm is the tire print). The load was applied and maintained at a rate of 2 mm / minutes and the load – deformation data were recorded until failure. The adopted failure criteria of asphalt concrete specimens were the drop in load and the punching deformation which is monitored by visual observation. A total of 18 specimens were prepared and tested duplicate while the average value of the test was considered for analysis. The accepted standard deviation between the strength and deformation values of each couple of specimens was 5 % and the average value of a minimum duplicate specimens was considered for the analysis for each testing condition.

3. Results and Discussions

3.1. Influence of geogrids on thin overlayer

Figure 4 demonstrates the positive influence of geogrids on the ability of the asphalt concrete to sustain the punching deformation of thin overlay of asphalt concrete with a thickness of 38.1 mm. It can be noticed that failure of the control samples occurs after 6 mm of punching deformation. However, the implication of AR-1 biaxial geogrid of 0.8 mm thickness and AR-G biaxial geogrid of 1.2 mm thickness as interlayer of asphalt concrete had provided a better ability to sustain the deformation at failure by (83.3 and 33.3) % respectively as compared with the control mixture. Such improvement could be attributed to restriction of the lateral and vertical movements of asphalt concrete ingredients due to the particle interlock provided by the aggregates inside the aperture of the geogrids. Larger aperture size of AR-G geogrid exhibits better ability of reinforced asphalt concrete to sustain punching deformation. Similar findings were reported by Mounes et al., 2016 [6]. The load

sustaining capacity at failure is 13 kN for control sample and decline to (10.5, and 10) kN when AR-1 and AR-G geogrids were implemented. Such a reduction in the load sustaining capacity of the reinforced asphalt concrete of (19.2, and 23) % as compared with the control asphalt concrete may be related to the higher stiffness of asphalt concrete structure created by the reinforcements which can control more deformation as compared with the control sample. Such a decline in the load carrying capacity of reinforced mixtures may also be attributed to the possible redistribution of the load configuration. More tensile stresses are created into the reinforced asphalt concrete to resist the creep of the mixture in the lateral direction while the shear stresses are resisting the punching deformation. Such a mechanism may explain the increase in the resistance to deformation and decline in the load carrying capacity. On the other hand, the viscoelastic stage of failure for control mixture ends after a punching deformation of 1 mm as demonstrated in Figure 4, while the viscoplastic stage of failure ends after a deformation of 6 mm. However, the reinforced asphalt concrete elastic stage of failure ends after a deformation of (8 and 11) mm for (AR-1 and AR-G) geogrids respectively, while the viscoplastic stage of failure was exhibited in the reduction in the load carrying capacity. A quick type of failure is exhibited in the control specimens while a more flexible type of failure could be observed in the reinforced specimens. Such failure mechanisms are typical as reported by Ibrahim et al, 2017 [1]; Zarei et al, 2025 [4].

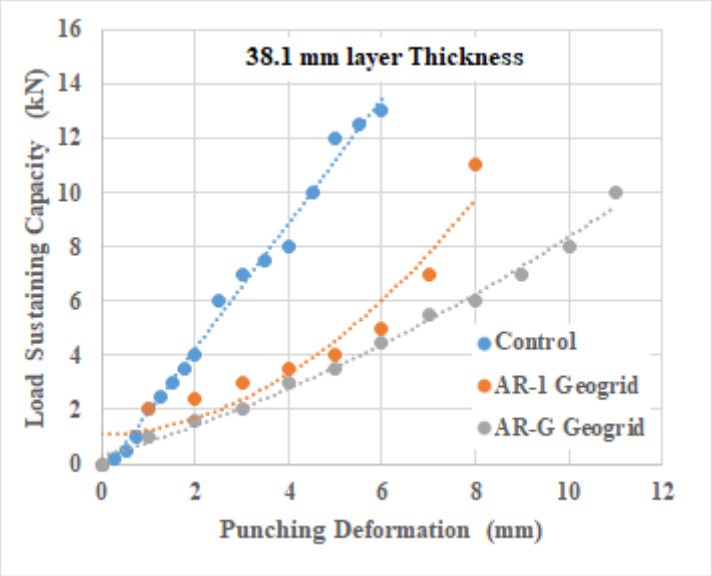

Figure 4. Influence of geogrids on deformation of thin asphalt concrete layer

Table 5 exhibits the mathematical models of deterioration of the control and reinforced asphalt concrete for the layer thickness of 38.1 mm. polynomial mathematical models with high coefficients of determination could be implemented to detect the sensitivity of asphalt concrete overlay thickness to implication of the geogrid reinforcements. It can be revealed that the viscoelastic stage of failure was extended and exhibited 6 mm of punching deformation when the geogrid reinforcements were implicated as interlayer as compared with the viscoelastic stage of failure of control sample which exhibits 1 mm of deformation. Zarei et al., 2025 [4] reported similar behavior. The choice of polynomial models was based on the high coefficient of determination (R^2) provided by each case, and the observed scatter of data.

Table 5. Deterioration models of control and reinforced asphalt concrete

Layer type	Deterioration model	R^2
Control	$Y = -0.0038 x^2 + 2.333 x - 0.414$	0.991
Reinforced with AR-1Geogrid	$Y = 0.1329 x^2 + 0.023 x + 1.104$	0.925
Reinforced with AR-G Geogrid	$Y = 0.0302 x^2 + 0.504 x + 0.294$	0.992

3.2. Influence of geogrids on thick overlay

Figure 5 demonstrates the influence of geogrids on the ability of the asphalt concrete to sustain the punching deformation of thick asphalt concrete layer of 63.5 mm thickness. It can be observed that failure of the control samples occurs after 2 mm of punching deformation. However, the implication of AR-1 biaxial geogrid of 0.8 mm thickness and AR-G biaxial geogrid of 1.2 mm thickness as interlayer of asphalt concrete had provided better ability to sustain the deformation at failure by 11.2 % regardless of the geogrid type as compared with the control mixture. Such minor improvement could be attributed to restriction of the lateral movement of asphalt concrete ingredients due to the particle interlock provided by the aggregates inside the aperture of the geogrids. The influence of the aperture size of geogrids was not significant due to the thicker pavement layer which eliminated the expected ability of reinforced asphalt concrete to sustain punching deformation. The load sustaining capacity at failure is 20 kN for control sample and decline to (12, and 10) kN when AR-1 and AR-G geogrids were implemented. Such a reduction in the load sustaining capacity of the reinforced asphalt concrete of (40, and 50) % as compared with the control asphalt concrete may be related to the possible non-homogeneity of asphalt concrete sample created by introducing the reinforcements which eliminate the positive influence of geogrids. The possibility of non-homogeneity of the mixture is related to implementation of grid at the interlayer within thick asphalt concrete overlay of 63.5 mm thickness and the rip thickness is (0.8 or 1.2) mm thickness. It is evident that asphalt concrete stability is highly sensitive to the position of the geogrids which provide integrity or separation of the mixture. On the other hand, the viscoelastic stage of failure for control mixture ends after a punching deformation of 0.5 mm as demonstrated in Figure 5, while the viscoplastic stage of failure ends after a deformation of 2 mm. However, the reinforced asphalt concrete elastic stage of failure ends after a deformation of 2.25 mm for both geogrids respectively, while the viscoplastic stage of failure was exhibited in the reduction in the load carrying capacity. A quick type of failure is exhibited in the control specimens while a more flexible type of failure with an extended viscoelastic stage of failure could be observed in the reinforced specimens. Such failure mechanisms are typical as reported by Ingrassia et al, 2020 [8]; Rueda et al, 2023 [19].

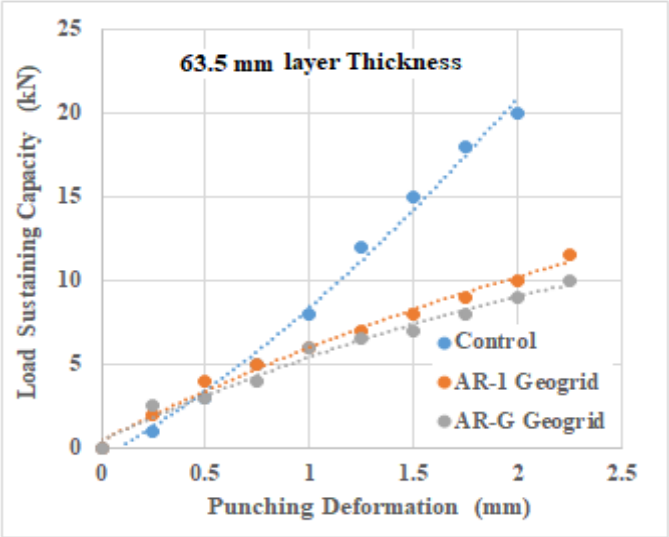

Figure 5. Influence of geogrids on deformation of thick asphalt concrete layer

Table 6 exhibits the mathematical models of deterioration of the control and reinforced asphalt concrete for the layer thickness of 63.5 mm. Polynomial mathematical models with high coefficients of determination could be implemented to detect the sensitivity of asphalt concrete overlay to the position of the geogrid reinforcements. Distinguishing the variation in the stages of failure was not significant among implementation of reinforcements into asphalt concrete mixture and the viscoplastic stage of failure ends after a punching deformation of (2 to 2.5) mm. Such findings agree with the work reported by Gallage et al., 2023 [12]; and Luan et al., 2923 [16].

Table 6. Deterioration models of control and reinforced asphalt concrete

Layer type	Deterioration model	R^2
Control	$Y= 1.7316\ x^2 + 7.336\ x - 0.678$	0.991
Reinforced with AR-1Geogrid	$Y= -0.6667\ x^2 + 6.215\ x + 0.445$	0.990
Reinforced with AR-G Geogrid	$Y= -0.6667\ x^2 + 5.621\ x + 0.463$	0.984

4. Conclusions

Based on the limited testing program and limitations of materials, the following remarks may be addressed:

- Implication of AR-1 biaxial geogrid and AR-G biaxial geogrid as interlayer of asphalt concrete had provided a better ability to sustain the deformation at failure by (83.3 and 33.3) % respectively as compared with the control mixture for thin layer of asphalt concrete.
- Larger aperture size of AR-G geogrid exhibits better ability of reinforced asphalt concrete to sustain punching deformation.
- The load sustaining capacity at failure declined by (19.2, and 23) % when AR-1 and AR-G geogrids were implemented as compared with the control asphalt concrete for thin layer of asphalt concrete.
- The viscoelastic stage of failure for thin layer of asphalt concrete was extended and exhibited 6 mm of punching deformation when the geogrid reinforcements were implicated as interlayer as compared with the viscoelastic stage of failure of control sample which exhibits 1 mm of deformation.
- For thick asphalt concrete layer, the implication of AR-1 and AR-G as interlayer had provided slightly better ability to sustain the deformation at failure by 11.2 % regardless of the geogrid type as compared with the control mixture.
- For thick asphalt concrete layer, the load sustaining capacity at failure declined by (40, and 50) % when AR-1 and AR-G geogrids were implemented as compared with the control asphalt concrete.
- Distinguishing the variation in the stages of failure was not significant among implementation of reinforcements into asphalt concrete mixture and the viscoplastic stage of failure ends after a punching deformation of (2 to 2.5) mm for thick pavement.
- Various overlay thickness, loading mode and rate, testing environment, and geogrid type are recommended for future testing programs.

Declaration of Conflict of Interests

The author declares that there is no conflict of interest. They have no known competing financial interests or personal relationships that could have appeared to influence the work reported in this paper.

References

[1.] Ibrahim E., El-Badawy S., Ibrahim N., Gabr A., Azam A. Effect of geogrid reinforcement on flexible pavements. Innovative Infrastructure Solutions, Springer International Publishing. December 2017. https://doi:10.1007/s41062-017-0102-7

[2.] Bekheet W., Ahmed R., Moussa G. Reinforcement of asphalt concrete layers using biaxial and triaxial geogrids, Conference Proceedings, The tenth Alexandria international conference on structural, geotechnical engineering and management AICSGE-10 December 2019.

[3.] Albayati, A. H.; Ajool, Y. S.; Allawi, A. A. Comparative Analysis of Reinforced Asphalt Concrete Overlays: Effects of Thickness and Temperature. MDPI Materials 2023, 16, 5990. https://doi.org/10.3390/ma16175990

[4.] Zarei S., Wang W., Ouyang J., Liu W. Failure mechanisms of geogrid-reinforced asphalt pavements: A viscoelastic 3D FEM analysis, Elsevier Construction and Building Materials, Volume 476, 2025, 141217, https://doi.org/10.1016/j.conbuildmat.2025.141217

[5.] Albayati A., Oukaili N., Obaidi H., Alatta B. Mitigating Reflection Cracking in Asphalt Concrete Overlays with ECC and Geotextile. Engineering, Technology & Applied Science Research Vol. 14, No. 1, February 2024, 12850-12860. https://doi:10.48084/etasr.6650

[6.] Mounes S., Karim M., Khodaii A., Almasi M. Evaluation of permanent deformation of geogrid reinforced asphalt concrete using dynamic creep test. Elsevier Geotextiles and Geomembranes, Volume 44, Issue 1, 2016, P. 109-116, https://doi.org/10.1016/j.geotexmem.2015.06.003

[7.] Solatiyan E., Bueche N., Alan Carter A. Laboratory evaluation of interfacial mechanical properties in geogrid-reinforced bituminous layers. Elsevier Geotextiles and Geomembranes, Volume 49, Issue 4, 2021, P. 895-909, https://doi.org/10.1016/j.geotexmem.2020.12.014

[8.] Ingrassia L., Virgili A., Canestrari F. Effect of geocomposite reinforcement on the performance of thin asphalt pavements: Accelerated pavement testing and laboratory analysis. Elsevier Case Studies in Construction Materials, Volume 12, 2020, e00342, https://doi.org/10.1016/j.cscm.2020.e00342

[9.] Kumar V., Roodi G., Subramanian S., Zornberg J. Influence of asphalt thickness on performance of geosynthetic-reinforced asphalt: Full-scale field study. Elsevier Geotextiles and Geomembranes, Volume 50, Issue 5, 2022, P. 1052-1059, https://doi.org/10.1016/j.geotexmem.2022.06.005

[10.] Kumar V., Saride S., Zornberg J. Fatigue performance of geosynthetic-reinforced asphalt layers, Emerald publishing, Geosynthetics International, Volume 28, Issue 6, 2021, P. 584-597, https://doi.org/10.1680/jgein.21.00013

[11.] Xue J., Gallage C., Qiu H., Zhong J., Southon A. Uncertainties in determining the responses of reinforced flexible pavements using in-situ tests, Elsevier Geotextiles and Geomembranes, Volume 51, Issue 5, 2023, P. 17-26, https://doi.org/10.1016/j.geotexmem.2023.04.010

[12.] Gallage, C., Wimalasena, K., Pathirana, A. Use of Geosynthetics for Sustainable, Economical, and Durable Road Pavement Structures. Proceedings of the 14th International Conference on Sustainable Built Environment. ICSBE 2023. Lecture Notes in Civil Engineering, vol 517. Springer, 2024. Singapore. https://doi.org/10.1007/978-981-97-3737-6_44

[13.] Sarsam S. Deformation Characteristics of Textile and Grid Reinforced Asphalt Concrete Pavement Model. Sciknow Publications Ltd. RAM (2013), 1(5): P. 49-55. Research and Application of Material https://www.researchgate.net/publication/275570646

[14.] Prakash, K., Rathod, D. Role of Geogrids and Geofoams as Interlayers in Pavement Foundation System: A Review. Springer nature, Int. J. Pavement Res. Technol. 2024. https://doi.org/10.1007/s42947-024-00475-3

[15.] Kumar V., Saride S., Zornberg J. Behavior of Asphalt Overlays with Geogrids and Geocomposite Interlayer Systems. Advances in Transportation Geotechnics IV Publisher: Springer, Cham January 2022 http://doi:10.1007/978-3-030-77234-5_50

[16.] Luan Y., Zhang W., Ma T., Cao J., Shi X., Tong Z. Effect of existing pavement condition and overlaying strategy on the reflective cracking resistance of asphalt pavement, Construction and Building Materials, Volume 401, 2023, 132620, https://doi.org/10.1016/j.conbuildmat.2023.132620

[17.] Patil C., and Shivananda P. Effect of axial stiffness of geogrid in the flexible pavement deformation through finite element analysis with Plaxis 2D. Journal of Emerging Technologies and Innovative Research (JETIR) JETIR, Volume 4, Issue 11, P. 375-379. November 2017. www.jetir.org

[18.] Asadi S., and Shafabakhsh G. Experimental and statistical investigation on the performance of asphalt overlays reinforced with geocomposite in controlling the reflective cracks under different loadings and temperatures. Applied Sciences 5(8). July 2023, SN http://doi:10.1007/s42452-023-05417-5.

[19.] Rueda, E.; Bastidas-Martínez, J.; Ruge, C.; Alayón, Y.; Olivos, J. Laboratory Analysis of an Asphalt Mixture Overlay Reinforced with a Biaxial Geogrid. MDPI Coatings 2023, 13, 99. https://doi.org/10.3390/coatings13010099

[20.] ASTM. Road and Paving Materials, Annual Book of ASTM Standards, Volume 04.03, American Society for Testing and Materials. West Conshohocken, USA. 2015. www.astm.com

[21.] SCRB. State Commission of Roads and Bridges. Standard Specification for Roads & Bridges, R-9 Asphalt concrete. Ministry of Housing & Construction, Baghdad-Iraq. 2003.

How to Cite This Article

Sarsam S. I. Sensitivity of Asphalt Overlay Thickness to Implication of Geogrids Reinforcement. Brilliant Engineering 2(2025), 41007. https://doi.org/10.36937/ben.2025.41007